ISSN 1070-3284, Russian Journal of Coordination Chemistry, 2015, Vol. 41, No. 4, pp. 285–292. © Pleiades Publishing, Ltd., 2015.

Synthesis and Structural Determination of Mononuclear Nine-Coordinate $(EnH_2)[Yb^{III}(Egta)(H_2O)]_2 \cdot 6H_2O$ and $[Yb^{III}(Eg3a)(H_2O)_2] \cdot 6H_2O$[1]

C. Qin, D. Y. Kong, and J. Wang*

Department of Chemistry, Liaoning University, Shenyang, 110036 P.R. China

**e-mail: wangjuncomplex890@126.com*

Received October 20, 2014

Abstract—Two novel rare earth metal coordination complexes, $(EnH_2)[Yb^{III}(Egta)(H_2O)]_2 \cdot 6H_2O$ (**I**) and $[Yb^{III}(Eg3a)(H_2O)_2] \cdot 6H_2O$ (**II**), where En = ethylenediamine, H_4Egta = ethyleneglycol-bis-(2-aminoethylether)-*N*,*N*,*N*',*N*'-tetraacetic acid and H_3Eg3a = ethyleneglycol-bis-(2-aminoethylether)-*N*,*N*,*N*'-triacetic acid, have been successfully synthesized through direct heating reflux and natural transformation. Complexes **I**, **II** were characterized by single-crystal X-ray diffraction techniques (CIF files CCDC nos. 966211 (**I**) and 966210 (**II**)). X-ray diffraction reveals that **I** is a nine-coordinate structure with a monocapped square antiprism crystallizing in the monoclinic crystal system with $P2_1/c$ space group. The cell dimensionsare: a = 12.9616(14) Å, b = 12.7134(13) Å, c = 15.0132(15) Å, β = 105.3720(10)° and V = 2385.5(4) Å^3. Complex **II** is also mononuclear nine-coordinate and crystallizes in the monoclinic crystal system with space group $P2_1/c$. The cell dimensions are as follows: a = 9.1926(10), b = 10.0046(12), c = 23.536(2) Å, β = 98.9650(10)° and V = 2385.5(4) Å^3. However, when **I** is continued to direct heating reflux, the octadentate Egta ligand losts an acetic acid group and becomes a heptadentate Eg3a ligand. Thus, **II** was obtained, which was confirmed by means of single crystal X-ray diffraction analysis. This finding may offer a fast and efficient one-step reaction synthesis method of asymmetric aminopolycarboxylic acid.

DOI: 10.1134/S1070328415040041

INTRODUCTION

The rare-earth metals (REMs) and their corresponding complexes have always been a rapid growing area over the past years owing to their applications of function materials, preparations of special catalysts, research and development of new medicines, and other aspects [1–9]. Particularly, some Tb(III) complexes with aminopolycarboxylic acid ligands have unusual spectroscopic characteristics including millisecond excited-state lifetime, sharply spiked emission spectra (few nm), and large Stokes shifts (>150 nm), so that they have been used as probes in fluoroimmunoassay [10, 11] and show considerable promise in luminescence imaging and as sensors for certain bioactive ions [12]. Some Gd(III) complexes are used as contrast agents for magnetic resonance imaging (MRI) diagnoses since there are seven high-spin singleelectrons in the *f* orbits of Gd(III), the most in all the REM ions [13–20]. In addition, Eu(III) complexes are promising for light-emitting layers of electroluminescent devices [21–23]. What's more, REM complexes exhibit effective catalytic activities. $[(Me_3Si)_2NC(NPri)_2]_2Sm(BH_4)_2Li(Thf)_2$ presents high catalytic activity for the application in polymerization of methyl methacrylate [24]. The addition of rare earth elements to catalysts has been performed mainly to enhance thermal stability of the catalysts themselves [25, 26]. High energy β-emitter of Y(III) represents significant superiority in the treatment of larger tumor [27, 28]. Recently, many researchers have focused on the Yb(III) complexes for their interesting properties. Ytterbium-doped lutetium pyrosilicate ($Yb:Lu_2Si_2O_7$) was reported to be suitable for the low-threshold and high-efficiency laser output [29]. Therefore, it is of great necessity to determine the crystal structure and geometrical configuration of Yb(III) complexes for further application.

In general, REM ions can form eight-, nine- and ten-coordinate complexes with various aminopolycarboxylic acid ligands, which depends on the ionic radius, electronic configuration and oxidation state of the central metal ion. We have worked hard in this field and reported a series of Yb(III) complexes with Nta (H_3Nta = nitrilotriacetic acid) and Egta (H_4Egta = ethyleneglycol-bis-(2-aminoethylether)-*N*,*N*,*N*',*N*'-tetraacetic acid) ligands by our laboratory. For Yb^{3+} ion, with the critical ionic radius of 1.008 Å, the chances of forming eight- and nine-coordinate complexes are equivalent. For instance, both $K_3[Yb^{III}(Nta)_2] \cdot 5H_2O$ and $Na_3[Yb^{III}(Nta)_2] \cdot 5H_2O$ adopt eight-coordinate structures with a pseudo-square antiprism [30], while the $[Yb^{III}(Nta)_2(H_2O)]^{3-}$

---

[1] The article is published in the original.

in $K_3[Yb^{III}(Nta)_2(H_2O)] \cdot 5H_2O$ [31] adopts a nine-coordinate monocapped square antiprism. We previously reported the complexes of $[Yb^{III}(HEgta)] \cdot 2H_2O$ [32] and $[Yb^{III}(HEgta)] \cdot 4H_2O$ [33] and found that they both adopt an eight-coordinate square antiprism. Although two complexes of $[Yb^{III}(HEgta)] \cdot 2H_2O$ and $[Yb^{III}(HEgta)] \cdot 4H_2O$ have protonated carboxyl O atoms, whereas the former is non-coordinated protonated carboxyl O atom, the latter is coordinated protonated carboxyl O atom. Therefore, the coordination number that Yb(III) selects is mainly associated with the shape of ligand and the coordinate environment. For most aminopolycarboxylic acid ligands, a rigid ring or a protonated carboxyl group fixes the conformation of REM complexes. Comparing with normal ligands, such complexes should have a great chance in forming low-coordinate structures.

In this work, for enriching the number and kind of aminopolycarboxylic acid compounds, a novel REM complex with Egta ligand, namely $(EnH_2)[Yb^{III}(Egta)(H_2O)]_2 \cdot 6H_2O$ (**I**), where En = ethylenediamine, was synthesized. As expected, it adopts nine-coordinate monocapped square antiprisms (MCSAP) with monoclinic space group $P2_1/n$. However, **I** is different from previously reported Yb(III) complexes with aminopolycarboxylic acid ligands. They have not protonated carboxyl O atoms. Unexpectedly, in reaction process along with further direct heating reflux, due to the presence of REM ions (Yb^{3+}) the octadentate Egta ligand loses an acetic acid group, and became a heptadentate Eg3a ligand, forming $[Yb^{III}(Eg3a)(H_2O)_2] \cdot 6H_2O$ (**II**). So, it can be conjectured that the symmetric H_4Egta in the presence of REM ions (Eu^{3+}, Tb^{3+}, and Yb^{3+}) loses an acetic acid group and becomes the asymmetric H_3Eg3a ligand. Perhaps, this method can be applied to synthesis of other asymmetric aminopolycarboxylic acid compounds. Thus, the decarboxylation reaction of H_4Egta caused by some REM ions will open up a new approach for the synthesis of H_3Eg3a.

EXPERIMENTAL

Materials and methods. Yb_2O_3 powder (99.999%, Yuelong Rare Earth Co., Ltd., China) and HEgta ligand (A.R., Beijing SHLHT Science and Trade Co., Ltd., China) were used to synthesis of aminopolycarboxylic acid complexes. In addition, ethanediamine and $NaHCO_3$ aqueous solutions were slowly add to solution in order to the pH was adjusted to 6.0. The structure of complexes were detected by X-ray (XT-V130, Beijing Xinzhuo Company, China) equipment.

Synthesis of I. H_4Egta (A.R., Beijing SHLHT Science and Trade Co., Ltd., China) (1.9017 g, 5.00 mmol) was added to 100 mL warm water and Yb_2O_3 powder (99.999%, Yuelong Rare Earth Co., Ltd., China) (0.9852 g, 2.50 mmol) was slowly added to above solution. The solution became transparent after the mixture had been stirred and refluxed for 15 h, and then the pH value was adjusted to 6.0 by dilute En aqueous solution. Finally, the solution was concentrated to 25.00 mL and placed in dark desiccator. A colorless crystal appeared after three weeks at room temperature.

Synthesis of II. The amount of reaction and reaction conditions were same as to above. However, the difference is that the reaction continues by direct heating reflux after synthesying complex **I**. And then, the pH value was also adjusted to 6.0 by dilute $NaHCO_3$ aqueous solution. Finally, the solution was concentrated to 25 mL and placed in dark desiccator. A light yellow crystal appeared after two weeks at room temperature.

X-ray structure determination. X-ray intensity data of **I** and **II** samples were collected on a Bruker SMART CCD type X-ray diffractometer system with graphite-monochromatized MoK_α radiation (λ = 0.71073 Å) at 298(2) K using φ–ω scan technique in the range of $1.72° \le \theta \le 26.00°$. Their structures were solved by direct methods. All non-hydrogen atoms were refined anisotropically by full-matrix least-squares methods. All the calculations were performed by the SHELXTL-97 program on PDP11/44 and Pentium MMX/166 computers. The crystal data and structure refinement for two complexes were listed in Table 1. And the selected bond distances and bond angles of two complexes were listed in Table 2.

Supplementary material has been deposited with the Cambridge Crystallographic Data Centre (nos. 966211 (**I**) and 966210 (**II**); deposit@ccdc.cam.ac.uk or http://www.ccdc.cam.ac.uk).

RESULTS AND DISCUSSION

It can be seen from Fig. 1a the central Yb^{3+} ion forms a 1 : 1 complex with H_4Egta, but its molecular and crystal structures is also somewhat different from that previously reported, for instance $[Yb^{III}(HEgta)] \cdot 2H_2O$ [32] and $[Yb^{III}(HEgta)] \cdot 4H_2O$ [33]. The molecular structure of $[Yb^{III}(Egta)(H_2O)]^-$ complex anion in **I** is shown in Fig. 1a. The Yb^{3+} ion is coordinated with one H_4Egta ligand by two amine nitrogen atoms, two ethyleneglycol oxygen atoms and four carboxylic oxygen atoms, which come from the same Egta ligand, and another oxygen atom from water molecules. It is similar to previously reported complexes, one water molecule is needed to coordinate to central Yb^{3+} ion forming complex **I** in addition to the Egta ligand. The two N atoms and six O atoms of one Egta ligand create seven five-membered chelating rings with the central Yb(1) ion, in which the four atoms are almost coplanar in each ring. It gives some similar findings previously reported, for instance $(EnH_2)[Sm^{III}(Egta)(H_2O)]_2 \cdot 6H_2O$ [34], $(EnH_2)[Ho^{III}(Egta)(H_2O)]_2 \cdot 6H_2O$ [35], $(EnH_2)[Eu^{III}(Egta)(H_2O)]_2 \cdot 6H_2O$ [36] and $(EnH_2)[Er^{III}(Egta)(H_2O)]_2 \cdot 6H_2O$ [37].

Table 1. Crystal data and structure refinement for **I** and **II**

Parameter	Value	
	I	**II**
Empirical formula	$C_{30}H_{66}N_6O_{28}Yb_2$	$C_{12}H_{33}N_2O_{15}Yb$
Formula weight	1304.97	618.44
Crystal system	Monoclinic	Monoclinic
Space group	$P2_1/c$	$P2_1/c$
Unit cell dimensions:		
a, Å	12.9616(14)	9.1926(10)
b, Å	12.7134(13)	10.0046(12)
c , Å	15.0132(15)	23.536(2)
β, deg	105.3720(10)	98.9650(10)
Volume, $Å^3$	2385.5(4)	2138.1(4)
Z	2	4
ρ_{calcd}, mg/m^3	1.817	1.921
Absorption coefficient mm^{-1}	3.992	4.450
F(000)	1304	1236
Crystal size, mm	0.25 × 0.21 × 0.10	0.49 × 0.40 × 0.39
θ Range for data collection, deg	2.13–25.02	1.75–25.02
Limiting indices	$-14 \leq h \leq 15$, $-15 \leq k \leq 13$, $-17 \leq l \leq 14$	$-10 \leq h \leq 10$, $-11 \leq k \leq 11$, $-26 \leq l \leq 28$
Reflections collected	11813	10392
Independent reflections (R_{int})	4205 (0.0732)	3762 (0.0352)
Completeness to θ_{max}, %	99.8	99.8
Max and min transmission	0.6910 and 0.4352	0.2757 and 0.2191
Goodness-of-fit on F^2	1.045	1.095
Final R indices ($I > 2\sigma(I)$)	$R_1 = 0.0452$, $wR_2 = 0.0991$	$R_1 = 0.0330$, $wR_2 = 0.0830$
R indices (all data)	$R_1 = 0.0675$, $wR_2 = 0.1081$	$R_1 = 0.0415$, $wR_2 = 0.0877$
Largest difference peak and hole, $e\ Å^{-3}$	2.102 and –1.013	1.004 and –1.053
Absorption correction	Empirical	

As seen from Fig. 2a, the coordination sphere around Yb(1) is similar to previously complexes, which can be best described as an nine-coordinate MCSAP conformation. The one square plane is formed by three carboxyl O atoms (O(3), O(5) and O(9)) and one ethyleneglycol O atom (O(1)). The opposite plane is formed by two carboxyl O atoms (O(7) and O(10), one ethyleneglycol O atom (O(2)) and one amine N atom (N(2)). The capping donor is occupied by one amine nitrogen atom (N(1)). In addition, as seen from Fig. 2a, because of the repulsion between the capped atoms (N(2)) and the bottom plane (O(1), O(3), O(5) and O(9)), the $Yb(1)N_2O_7$ part is not standard MCSAP. For the top plane, the average value of the MCSAP angle between Δ(O(1)O(5)O(9)) and Δ(O(1)O(3)O(9)) is about 5.47°, and between Δ(O(1)O(3)O(5)) and Δ(O(3)O(5)O(9)) is about 5.95°. For the bottom plane, the average value of the MCSAP angle between Δ(O(2)N(2)O(10)) and Δ(N(2)O(7)O(10)) is about 0.17°, and between Δ(O(2)O(7)O(10)) and Δ(O(2)N(2)O(7)) is about 0.17°. According to these calculated data, we also can firmly draw a conclusion that the conformation of $Yb(1)N_2O_7$ in the $[Yb^{III}(Egta)(H_2O)]^-$ complex anion indeed keeps a MCSAP conformation but distort to a small extent.

The lengths of the Yb–O bond in **I** is in the wide range from 2.307 to 2.476(5) Å and the average value is about 2.289 Å. It is somewhat shorter than the corresponding value (2.333 to 2.544 Å) in **II**, which indicates that complex **I** is more stable than complex **II**. The Yb(1)–N bond distances vary from 2.613 to 2.626 Å, respectively with the average value of 2.661 Å; they are remarkably longer than the Yb(1)–O bond

Table 2. Selected bond distances (w) and angles (deg) of **I** and **II**

Bond	*d*, Å	Bond	*d*, Å	Bond	*d*, Å
			I		
Yb(1)–O(1)	2.464(5)	Yb(1)–O(5)	2.312(5)	Yb(1)–O(11)	2.424(5)
Yb(1)–O(2)	2.476(5)	Yb(1)–O(7)	2.307(6)	Yb(1)–N(1)	2.626(6)
Yb(1)–O(3)	2.323(5)	Yb(1)–O(9)	2.319(5)	Yb(1)–N(2)	2.613(6)
			II		
Yb(1)–O(1)	2.529(4)	Yb(1)–O(5)	2.333(4)	Yb(1)–O(10)	2.441(4)
Yb(1)–O(2)	2.544(4)	Yb(1)–O(7)	2.377(4)	Yb(1)–N(1)	2.648(5)
Yb(1)–O(3)	2.344(4)	Yb(1)–O(9)	2.397(4)	Yb(1)–N(2)	2.566(5)
Angle	ω, deg	Angle	ω, deg	Angle	ω, deg
			I		
O(1)Yb(1)O(2)	67.85(18)	O(2)Yb(1)O(11)	65.27(17)	O(5)Yb(1)N(1)	66.19(18)
O(1)Yb(1)O(3)	128.90(18)	O(2)Yb(1)N(1)	130.50(19)	O(5)Yb(1)N(2)	144.3(2)
O(1)Yb(1)O(5)	88.87(19)	O(2)Yb(1)N(2)	67.57(18)	O(7)Yb(1)O(9)	131.63(18)
O(1)Eu(1)O(7)	135.81(19)	O(3)Yb(1)O(5)	89.39(19)	O(7)Yb(1)O(11)	73.52(18)
O(1)Yb(1)O(9)	72.91(19)	O(3)Yb(1)O(7)	79.50(18)	O(7)Yb(1)N(1)	129.6(2)
O(1)Yb(1)O(11)	75.98(19)	O(3)Yb(1)O(9)	77.21(19)	O(7)Yb(1)N(2)	66.99(19)
O(1)Yb(1)N(1)	67.82(19)	O(3)Yb(1)O(11)	148.23(19)	O(9)Yb(1)O(11)	133.86(18)
O(1)Yb(1)N(2)	126.31(19)	O(3)Yb(1)N(1)	64.97(18)	O(9)Yb(1)N(1)	75.18(19)
O(2)Yb(1)O(3)	137.32(18)	O(3)Yb(1)N(2)	73.39(19)	O(9)Yb(1)N(2)	65.94(19)
O(2)Yb(1)O(5)	132.86(17)	O(5)Yb(1)O(7)	79.49(19)	O(11)Yb(1)N(1)	122.14(19)
O(2)Yb(1)O(7)	99.91(19)	O(5)Yb(1)O(9)	141.19(18)	O(11)Yb(1)N(2)	109.84(18)
O(2)Yb(1)O(9)	71.78(17)	O(5)Yb(1)O(11)	69.65(18)	N(1)Yb(1)N(2)	127.87(19)
			II		
O(1)Yb(1)O(2)	64.39(14)	O(2)Yb(1)O(10)	69.58(15)	O(5)Yb(1)N(1)	66.08(14)
O(1)Yb(1)O(3)	91.85(15)	O(2)Yb(1)N(1)	120.09(14)	O(5)Yb(1)N(2)	74.42(16)
O(1)Yb(1)O(5)	76.44(15)	O(2)Yb(1)N(2)	66.72(15)	O(7)Yb(1)O(9)	77.33(15)
O(1)Yb(1)O(7)	141.68(14)	O(3)Yb(1)O(5)	130.25(14)	O(7)Yb(1)O(10)	70.79(15)
O(1)Yb(1)O(9)	137.99(14)	O(3)Yb(1)O(7)	78.78(14)	O(7)Yb(1)N(1)	136.34(15)
O(1)Yb(1)O(10)	70.95(15)	O(3)Yb(1)O(9)	79.99(14)	O(7)Yb(1)N(2)	64.92(16)
O(1)Yb(1)N(1)	66.09(14)	O(3)Yb(1)O(10)	78.74(15)	O(9)Yb(1)O(10)	144.43(15)
O(1)Yb(1)N(2)	128.75(16)	O(3)Yb(1)N(1)	65.01(14)	O(9)Yb(1)N(1)	73.24(14)
O(2)Yb(1)O(3)	145.01(14)	O(3)Yb(1)N(2)	138.76(15)	O(9)Yb(1)N(2)	73.77(15)
O(2)Yb(1)O(5)	71.38(14)	O(5)Yb(1)O(7)	136.82(14)	O(10)Yb(1)N(1)	121.30(15)
O(2)Yb(1)O(7)	103.54(14)	O(5)Yb(1)O(9)	77.99(14)	O(10)Yb(1)N(2)	105.35(16)
O(2)Yb(1)O(9)	134.92(14)	O(5)Yb(1)O(10)	136.97(14)	N(1)Yb(1)N(2)	132.54(16)

distances. So, the O atoms coordinate to the central Yb^{3+} ion much stronger than the N atoms. The OYb(1)O bond angles change from 65.27° to 148.23°. The OYb(1)N bond angles vary from 64.97° to 144.3°, and the N(1)YbN(2) bond angle is 127.87°. Thus, as shown above, the coordination polyhedron around the Yb^{3+} ions in complexes **I** and **II** are similar to each other, although there are some differences in the bond lengths and bond angles between two complex molecules.

As seen from Fig. 3a, there are two molecules in one unit cell of **I**. The complex molecules connect with one another through hydrogen bonds and electrostatic forces with crystallization water and protonated ethylenediamine cation (EnH_2^{2+}). Furthermore, the hydrogen bonds play an important role in the

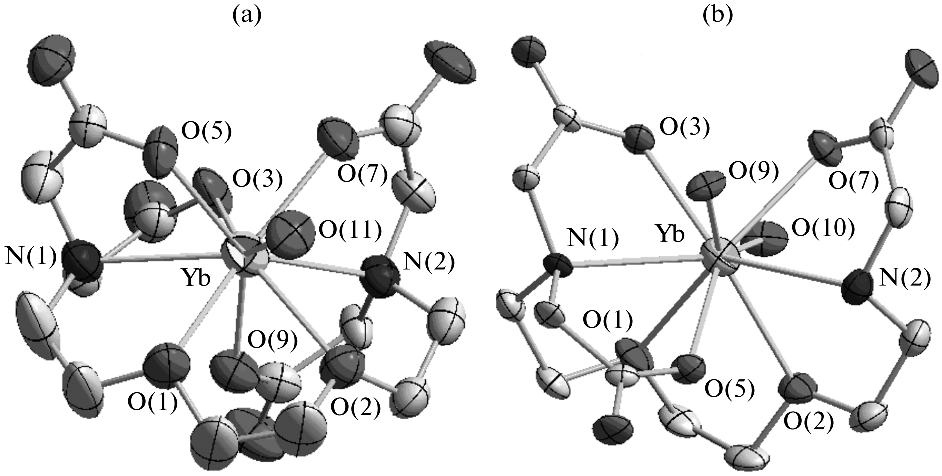

Fig. 1. Molecular structures of **I** (a) and **II** (b).

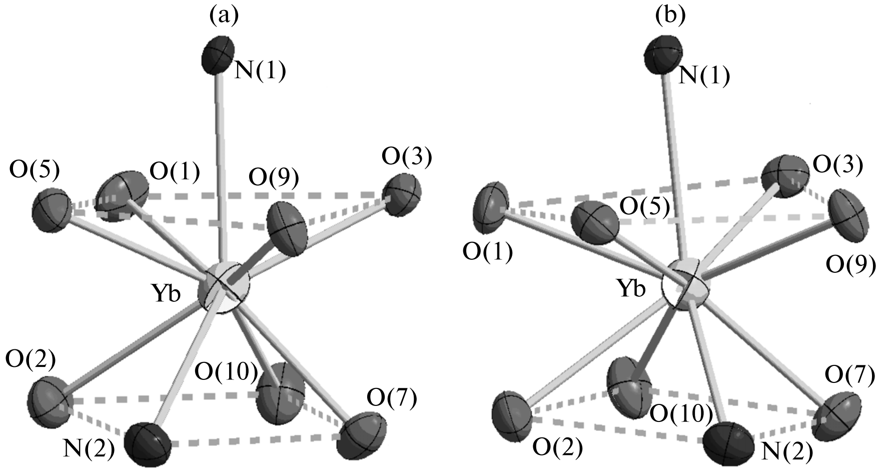

Fig. 2. Coordination polyhedron around Yb^{3+} ion in **I** (a) and **II** (b).

structure of complex **I**. As shown in Fig. 4 and Table 3, an EnH_2^{2+} cation forms the hydrogen bonds with three adjacent $[Yb^{III}(Egta)(H_2O)]^-$ complex anions. Obviously, the EnH_2^{2+} cation is located in a centrosymmetric structure. That is, N(3) and N(8) both connect with three carboxyl O atoms, in which O(4), O(6), and O(8) come from three carboxyl group of neighboring $[Yb^{III}(Egta)(H_2O)]^-$ complex anions. The distances of N(3)···O(4), N(3)···O(6) and N(3)···O(8) are 2.796, 2.801 and 2.762 Å, respectively, resulting in formation of infinite 1D chains. As shown in Fig. 5, two 1D chains are linked by sharing ethylenediamine (N(3)–C(16)–C(16)–N(8)) in theacplane leading to the for-

Table 3. Geometric parameters of hydrogen bonds of **I**

D–H···A	Distance, Å			Angle DHA, deg	Symmetry code
	D–H	H···A	D···A		
N(3)–H(3*A*)···O(8)	0.89	1.89	2.762	166	$x, y-1, z$
N(3)–H(3*B*)···O(6)	0.89	1.93	2.801	166	$-x+1, -y+1, -z+1$
N(3)–H(3*B*)···O(5)	0.89	2.65	3.083	111	$-x+1, -y+1, -z+1$
N(3)–H(3*C*)···O(4)	0.89	1.91	2.796	177	$-x+3/2, y-1/2, -z+3/2$

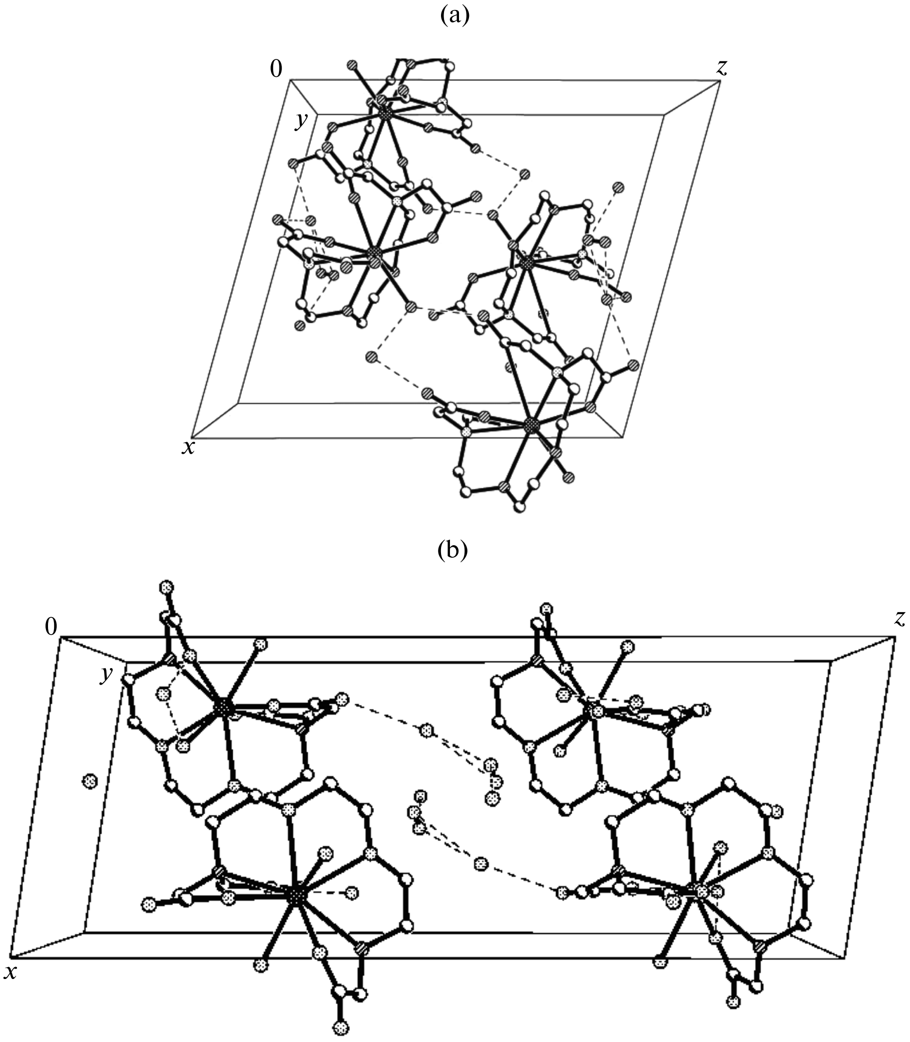

Fig. 3. Arrangement of **I** (a) and **II** (b) in unit cell (dashed lines represent intermolecular hydrogen bonds).

mation of a close-knit 2D ladder-like network. Owing to this special coordination environment, the Newman projection pattern dihedral angle of ethylenediamine is exactly 180°. Four non-hydrogen atoms of ethylenediamine all locate in the same plane. Therefore, it can be observed that amino acids can interact with the $[Yb^{III}(Egta)(H_2O)]^-$ complex anion through different binding manner.

It can be seen evidently from Fig. 1b complex **II** has a mononuclear molecular structure, but its molecular and crystal structures is also somewhat different from complex **I**. The centre metal Yb^{3+} ion is in a nine-coordinated environment with five carboxyl O atoms (O(1), O(2), O(3), O(5) and O(7)) from one octadentate Eg3a ligand, two amine N atoms (N(1) and N(2)) and two other O atoms (O(9) and O(10)) from water molecules. The two N atoms and five O atoms of one Eg3a ligand create six five-membered chelating rings with the central Yb(1) ion, in which the four atoms are almost coplanar in each ring. It is worth reminding that the used octadentate Egta ligand from complex **I** has lost an acetic acid group and become a heptadentate Eg3a ligand of complex **II** as shown in Fig. 1a.

As we predicted, complex **II** adopts an nine-coordinate structure with MCSAP conformation (Fig. 2b). The upper square plane is formed by one ethyleneglycol O atom (O(1)), two carboxyl O atoms (O(3) and O(5)) and one water O atom (O(9)), and the nether plane is formed by one amine N atom (N(2)), one ethyleneglycol O atom (O(2)), one carboxyl O atoms (O(7)) and one water O atom (O(10)). The capping donor is occupied by one amine nitrogen atom (N(1)). The torsion angle between the two (upper and nether) quadrilateral planes is about 50.61°. Otherwise, from Fig. 2b, the values about MCSAP angle as the confirmation standard can be calculateed. For the upper quadrilateral plane, the average value of the trigonal dihedral angle between Δ(O(1)O(3)O(5)) and Δ(O(3)O(5)O(9)) is about 5.95°, and between Δ(O(1)O(3)O(9)) and Δ(O(1)O(5)O(9)) is about

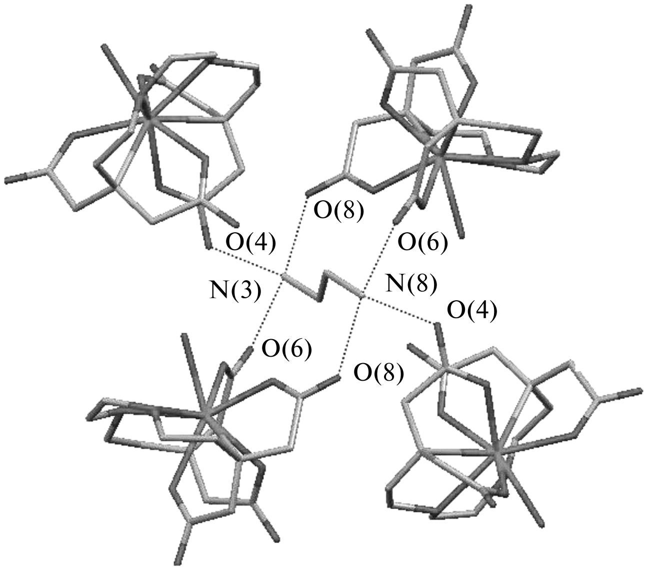

Fig. 4. Bindings between EnH_2^{2+} and $[Yb^{III}(Egta)(H_2O)]^{2-}$ in **I** (a) (dashed lines represent intermolecular hydrogen bonds).

6.47°. For the bottom plane, the value of the dihedral angle between Δ(O(2)N(2)O(10)) and Δ(O(7)N(2)O(10)) triangles is 0.17°, and between Δ(O(2)O(7)O(10)) and Δ(O(2)O(7)N(2)) triangle is 0.17°. The judgment about a monocapped square antiprismatic polyhedron, according to Guggenberger and Muetterties'method [38], depends on the special bottom plane dihedral angle, which is apparently smaller than 26.40°. Therefore, although distorted, the $[Yb^{III}(Eg3a)]$ complex still retains a MCSAP polyhedron.

For complex **II**, the Yb–O bond distances range from 2.333 to 2.544 Å, and the average value is about 2.2893 Å (Table 2). Furthermore, the bond distances of Yb(1)–O(1) and Yb(1)–O(2) (both belonging to ethyleneglycol O atoms) are somewhat longer than other Yb(1)–O bond lengths, which are 2.529 and 2.544 Å, respectively. Not surprisingly, it is consistent with the findings with H_4Egta ligands made by previously reported. This also indicates that the O atoms (O(3), O(5), and O(7)) from coordinate carboxylic groups form coordinate bonds more stably than the ethyleneglycol O atoms (O(1) and O(2)). While the bond distances between the central Yb^{3+} ion and O(9) and O(10) from the water molecules are both longer than the other Yb–O bond distances, which are 2.397 and 2.441 Å, respectively. It indicate that the Eg3a ligand coordinates with the Yb^{3+} ion more stably than the water molecules. In addition, the Yb(1)–O bond distances are significantly shorter than the Yb(1)–N bond distances, indicating that the Yb(1)–O bonds are much stronger than the Yb(1)–N bonds. In any case, the Yb(1)–O bond distances are significantly shorter than the Yb(1)–N bond distances. Consequently, all these lead to a distorted geometric configuration. Table 2 also illustrates a series of bond angles. The OYb(1)O bond angles in complex **II** are in the wide range from 64.39° to 145.01°, while the OYbN bond angles vary from 64.92° to 138.76° and the N(1)YbN(2) bond angle is 132.54°.

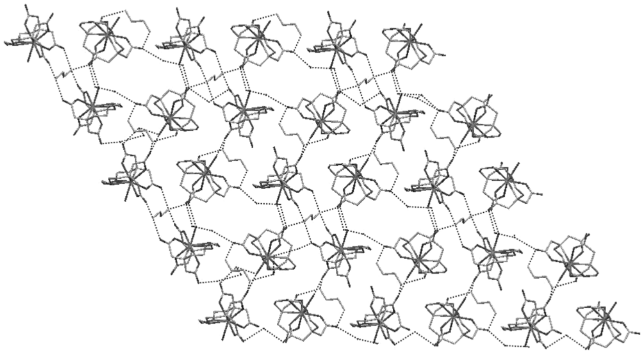

Fig. 5. Polyhedral view of the 2D ladder-like layered network of **II** (b).

In one unit cell of **II**, as seen from Fig. 3b, there are four complex molecules. Two adjacent molecules connect through hydrogen bonds and are associated with crystal waters. Therefore, a layer structure is formed through hydrogen bonds and electrostatic bondings.

ACKNOWLEDGMENTS

The authors greatly acknowledge the National Science Foundation of China (21371084), Innovation Team Project of Education Department of Liaoning Province (LT2012001), Public Research Fund Project of Science and Technology Department of Liaoning Province (2012004001), Shenyang Science and Technology Plan Project (F12-277-1-15 and F13-289-1-00) and Science Foundation of Liaoning Provincial Education Department (L2011007) for financial support. The authors also thank our colleagues and other students for their participating in this work.

REFERENCES

1. Ma, S., Sun, D., Wang, X.S., et al., *Angew. Chem. Int. Ed.*, 2007, vol. 46, p. 2458.
2. Cairns, A.J., Perm, J.A., Wojtas, L., et al., *J. Am. Chem. Soc.*, 2008, vol. 130, p. 1560.
3. Zhang, J.P. and Chen, X.M., *J. Am. Chem. Soc.*, 2008, vol. 130, p. 6010.
4. Lee, J.Y., Olson, D.H., Pan, L., et al., *Adv. Funct. Mater.*, 2007, vol. 17, p. 1255.
5. Alvaro, M., Carbonell, E., Ferrer, B., et al., *Chem. Eur. J.*, 2007, vol. 13, p. 5106.
6. Xue, M., Zhu, G.S., Li, Y.X., et al., *Cryst. Growth Des.*, 2008, vol. 8, p. 2478.
7. Yu, X.H., Seo, S.Y., and Marks, T.J., *J. Am. Chem. Soc.*, 2007, vol. 129, p. 7244.

8. Amin, S.B. and Marks, T.J., *J. Am. Chem. Soc.*, 2007, vol. 129, p. 10102.
9. Verbruggen, A.M., *J. Nucl. Med.*, 1990, vol. 17, p. 346.
10. Volkert, W.A., Goeckeler, W.F., Ehrhardt, G.J., et al., *J. Nucl. Med.,* 1991, vol. 32, p. 174.
11. Ozolinsh, M. and Eichler, H.J., *Appl. Phys. Lett.*, 2000, vol. 77, p. 615.
12. Terai, T., Kikuchi, K., Iwasawa, S., et al., *J. Am. Chem. Soc.,* 2006, vol. 128, p. 6928.
13. Teotonio, E.E.S., Brito, H.F., Felinto, M.C.F.C., et al., *J. Mol. Struct.*, 2005, vol. 751, p. 85.
14. Deshpande, S.V., Denardo, S.J., Kukis, D.L., et al., *J. Nucl. Med.*, 1990, vol. 31, p. 473.
15. Miao, Y.B., Hoffman, T.J., and Quinn, T.P., *Nucl. Med. Biol.*, 2005, vol. 32, p. 485.
16. Efthimiadou, E.K., Katsarou, M.E., Fardis, M., et al., *Bioorg. Med. Chem. Lett.*, 2008, vol. 18, p. 6058.
17. Kupriyanov, V., Yang, Y., Gervai, P., et al., *J. Mol. Cell. Cardiol.*, 2008, vol. 44, p. 715.
18. Accardo, A., Tesauro, D., Aloj, L., et al., *Coord. Chem. Rev.*, 2009, vol. 253, p. 2193.
19. Vaccaro, M., Accardo, A., Errico, G.D., et al., *Biophys. J.*, 2007, vol. 93, p. 1736.
20. Chong, H.S., Song, H.A., Lim, S., et al., *Bioorg. Med. Chem. Lett.,* 2008, vol. 18, p. 2505.
21. Weissleder, R. and Mahmood, U., *Radiology,* 2001, vol. 219, p. 316.
22. Hak, S., Sanders, H.M.H.F., Agrawal, P., et al., *Eur. J. Pharm. Biopharm.*, 2009, vol. 72, p. 397.
23. Huang, S.N., Liu, C., Dai, G.P., et al., *NeuroImage,* 2009, vol. 46, p. 589.
24. Egli, T., *J. Biosci. Bioeng.*, 2001, vol. 92, p. 89.
25. Sillanpää, M., Orama, M., Ramo, J., et al., *Sci. Total Environ.*, 2001, vol. 267, p. 23.
26. Rajesh, N.P., Meera, K., Perumal, C.K., et al., *Mater. Chem. Phys.*, 2001, vol. 71, p. 299.
27. Hak, S., Sanders, H.M.H.F., Agrawal, P., et al., *Eur. J. Pharm. Biopharm.*, 2009, vol. 72, p. 397.
28. Li, Z.F., Li, W.S., Li, X.J., et al., *Magn. Reson. Imaging*, 2007, vol. 25, p. 41.
29. Kubíček, V. and Tóth, É., *Adv. Inorg. Chem.*, 2009, vol. 61, p. 63.
30. Wang, J., Zhang, X.D., Zhang, Y., et al., *J. Struct. Chem.*, 2004, vol. 45, no. 1, p. 114.
31. Wang, J., Zhang, X.D., Jia, W.G., et al., *Chem. Res. Chin. Univ.*, 2003, vol. 19, p. 145.
32. Wang, J., Hu, P., Liu, B., et al., *J. Coord. Chem.*, 2009, vol. 62, p. 3168.
33. Gao, J.Q., Li, D., Wang, J., et al., *Russ. J. Coord. Chem.,* 2011, vol. 37, p. 473.
34. Gao, J.Q., Li, D., Wang, J., et al., *J. Coord. Chem.*, 2011, vol. 64, p. 2234.
35. Bai, Y., Gao, J.Q., Wang, J., et al., *Russ. J. Coord. Chem.*, 2013, vol. 39, p. 147.
36. Xu, R., Li, D., Wang, J., et al., *Russ. J. Coord. Chem.*, 2010, vol. 36, p. 810.
37. Gao, J.Q., Wu, T., Wang, J., et al., *Russ. J. Coord. Chem.*, 2011, vol. 37, p. 817.
38. Guggenberger, L.J. and Muetterties, E.L., *J. Am. Chem. Soc.*, 1976, vol. 98, p. 7221.